Density and Surface Tension of Ionic Liquids

C. Kolbeck,[†] J. Lehmann,[||] K. R. J. Lovelock,[†] T. Cremer,[†] N. Paape,[‡] P. Wasserscheid,[‡,§] A. P. Fröba,[||] F. Maier,*[,†] and H.-P. Steinrück[†,§]

Lehrstuhl für Physikalische Chemie II, Lehrstuhl für Chemische Reaktionstechnik, and Erlangen Catalysis Resource Center (ECRC), Universität Erlangen-Nürnberg, Egerlandstrasse 3, 91058 Erlangen, Germany, and Erlangen Graduate School in Advanced Optical Technologies (SAOT), Universität Erlangen-Nürnberg, Paul-Gordon-Strasse 6, 91052 Erlangen, Germany

Received: July 22, 2010; Revised Manuscript Received: November 15, 2010

We measured the density and surface tension of 9 bis[(trifluoromethyl)sulfonyl]imide ($[Tf_2N]^-$)-based and 12 1-methyl-3-octylimidazolium ($[C_8C_1Im]^+$)-based ionic liquids (ILs) with the vibrating tube and the pendant drop method, respectively. This comprehensive set of ILs was chosen to probe the influence of the cations and anions on density and surface tension. When the alkyl chain length in the $[C_nC_1Im][Tf_2N]$ series ($n = 1$, 2, 4, 6, 8, 10, 12) is increased, a decrease in density is observed. The surface tension initially also decreases but reaches a plateau for alkyl chain lengths greater than $n = 8$. Functionalizing the alkyl chains with ethylene glycol groups results in a higher density as well as a higher surface tension. For the dependence of density and surface tension on the chemical nature of the anion, relations are only found for subgroups of the studied ILs. Density and surface tension values are discussed with respect to intermolecular interactions and surface composition as determined by angle-resolved X-ray photoelectron spectroscopy (ARXPS). The absence of nonvolatile surface-active contaminants was proven by ARXPS.

1. Introduction

Ionic liquids (ILs)—salts with a melting point below 100 °C—have shown great promise in both experimental and theoretical environments in the past decade.[1] Due to their structural diversity, there is a nearly unlimited number of potential primary ILs (combination of one cation and one anion), many of which have very interesting physicochemical properties, leading to a burgeoning area of IL research and of applications of ILs[2] as lubricants,[3,4] in gas separation processes,[5,6] as gas storage media,[7,8] and as solvents in multiphasic catalysis,[9−11] and electrochemistry.[12−14] In many of these applications, the interface to the environment plays a vital role. Therefore, knowledge of interface properties, particularly of the surface and interfacial tension, and its relationship to the ILs' chemical nature is crucial to choose the right IL for a specific application.

In view of the large number of potentially interesting ILs, prediction methods for the physicochemical properties of new ILs are highly desirable. It has been reported by Krossing and co-workers that the molecular volume V_m, as derived from DFT calculations, is strongly correlated with the viscosity, conductivity, and density of ILs, which allows predictions for even unknown ILs with very good accuracy.[15] In order to verify the general applicability of this approach, it is necessary to provide large and consistent experimental data sets of V_m values of known ILs which are determined by accurate density measurements. Moreover, the investigation of the influence of specific chemical groups on the IL density contributes to the understanding of intermolecular interactions as it will be discussed later.

Previous studies[16] of the surface tension (ST) at the liquid/gas or liquid/vacuum interface of ILs can be broadly split into two categories: those varying the length of the alkyl chain on the cation and those varying the anion. With increasing alkyl chain length in the cation, a general trend toward lower ST values has been reported;[17−27] simulations have confirmed these experimental findings.[28,29] In a recent study, Santos et al. showed that ST of ILs decreases with increasing chain length independent of the chain being located on the cation or the anion.[25] Investigations involving the same cation and different anions have led to a variety of conclusions, e.g., relating the ST with the size and charge delocalization on the anion.[22,30−32] From their experimental findings, Law et al. proposed that, for a given cation, the ST of an IL generally increases with increasing anion size.[32] However, using a wider range of anions Martino et al. found no general trend with anion size.[33] An extensive set of ST values of $[C_2C_1Im]^+$-containing ILs has been published by Larriba et al., who concluded that interstitial void volumes described by a void function could be used to explain trends in ST values.[34] From experimental data, Freire et al. proposed that the ST decreases for ILs with increasing anion size, which was attributed to the higher charge delocalization in larger anions and, therefore, a decrease in hydrogen-bonding ability.[22] Summarizing surface and interface tension literature on ILs, it seems that simple trends were observed only in studies where a relatively small range of ILs had been employed. In many cases, the ST was solely related to intermolecular interactions being present in the bulk. However, the development of more general concepts for explaining and predicting ST across a large number of different ILs seems to be difficult, which could be related to the complex nature of ILs.

The reliable and accurate measurement of ST is not trivial. First of all, sample purity, especially the absence of surface active contaminations, is a critical issue. Second, ST data obtained using different methods (and by different research groups) often considerably deviate from each other in absolute values (note that relative trends are often well reproduced).

* Corresponding author. E-mail: florian.maier@chemie.uni-erlangen.de.
[†] Lehrstuhl für Physikalische Chemie II.
[‡] Lehrstuhl für Chemische Reaktionstechnik.
[§] Erlangen Catalysis Resource Center (ECRC).
[||] Erlangen Graduate School in Advanced Optical Technologies (SAOT).

10.1021/jp1068413
Published on Web 12/08/2010

Besides sample handling and preparation procedures, this unsatisfying data situation may be caused by the use of routine lab analytic methods, e.g., du Noüy tensiometers, which are often overestimated regarding the achievable accuracy.[35] Also, the margin of errors is often ignored or not stated in the existing ILs literature. For these reasons and to allow for a better understanding, a large data set of ILs measured with one reliable method is required.

The ST is defined as the change of surface free enthalpy G per area A ($\sigma = \delta G/\delta A$). As already pointed out by Irving Langmuir, the ST is closely related to the intermolecular interactions in the bulk (cohesive energy) and the molecular orientation at the surface.[36,37] According to the "principle of independent action between surfaces of molecules", which is also known as "Langmuir principle", these intermolecular interactions mainly depend on the nature of those chemical groups of the interacting molecules which are in contact with each other.[36] For liquids composed of spherical molecules with *isotropic* intermolecular interactions, strong cohesive energies in the bulk lead to high ST values. This relationship between bulk cohesive energy and ST is also a good approximation for liquids in which surface ordering effects are negligible. For liquids composed of nonspherical molecules with *nonisotropic* interactions with neighboring molecules, molecules very close to the surface can display a preferential orientation in order to minimize surface energy: chemical groups of the molecules, which are least attracted by neighboring molecules, preferentially point toward the gas/vacuum side whereas chemical groups most strongly attracted by their neighbors preferentially point toward the bulk. In this nonisotropic case, the liquid's surface does not represent a random truncation of the bulk but is mainly composed of the weakly interacting parts of the molecules. Within the framework of the Langmuir principle, the ST is given by the superposition of the contributions from only those chemical groups that form the outer surface (for isotropic case the outer surface is represented by a bulk truncation). One famous example already given by Langmuir is the ST of linear *n*-alkanols, where the hydrophilic hydroxyl groups mainly point to the bulk and the hydrophobic alkyl tails are mainly oriented away from the bulk and dominate the composition of the outermost molecular layer; thus, the ST values of the *n*-alkanols ($n > 5$) are close to the ST of the analogue *n*-alkane.[36] The two aspects for the observed ST, "bulk cohesive energy" and "molecular orientation", will be discussed in detail below in the context of IL surface composition, which was determined by angle resolved photoelectron spectroscopy (ARXPS). In contrast to ordinary liquids, the very low vapor pressure of ILs allow to apply this ultrahigh vacuum (UHV) based technique, and consequently to study liquid surfaces at an unprecedented molecular level.[38]

In this paper, we present data on the density and surface tension of 21 different ILs (Table 1), which were measured using the vibrating tube and the pendant drop method, respectively, under ambient conditions. These ILs can be divided in two groups. The first consists of ILs with the anion bis[(trifluoromethyl)sulfonyl]imide ($[Tf_2N]^-$). By systematic variation of the cation the dependence of the ST on the alkyl chain length at the imidazolium ring, the functionalization of this chain by ethylene glycol groups and modifications in the cationic head group are investigated. The second group consists of ILs with the cation 1-methyl-3-octylimidazolium ($[C_8C_1Im]^+$) to discuss the effect of the anion on density and ST. The chosen anions range from small anions (Cl^-, Br^-, $[NO_3]^-$, $[BF_4]^-$), medium-sized anions ($[MeOSO_3]^-$, $[TfO]^-$, $[PF_6]^-$, $[B(CN)_4]^-$) to large, weakly coordinating anions ($[Tf_2N]^-$, $[Pf_2N]^-$, $[FAP]^-$).

2. Experimental Section

Materials and Sample Preparation Procedure. $[C_nC_1Im][Tf_2N]$ ILs ($n = 1, 4, 6, 8, 10, 12$) were synthesized according to ref 39 and $[C_8C_1Im]Cl$ and $[C_8C_1Im][Pf_2N]$ according to ref 40. $[C_8C_1Im][MeOSO_3]$ was synthesized by a quaternization reaction of octylimidazole with dimethyl sulfate under solvent-free conditions. Precooling of the octylimidazole was important to yield a colorless product. $[Me(EG)_2C_1Im][Tf_2N]$ was synthesized by reacting $Me-EG_2-OH$ ($EG = -O-CH_2-CH_2-$) with benzenesulfonyl chloride to obtain the EG−benzenesulfonate. The latter was used to alkylate 1*H*-imidazole to form the EG-functionalized imidazole.[41] The IL was synthesized from functionalized imidazole by alkylation with iodomethane followed by ion exchange with $Li[Tf_2N]$.

All synthesized ILs were dried after preparation in vacuum (9×10^{-3} mbar) at 40 °C for 24 h. The purities of the samples were verified by ^1H NMR analysis (JEOL, ECX +400 spectrometer), with dimethyl sulfoxide-d_6 (DMSO-d_6) as solvent. The total peak integral in the ^1H NMR spectrum was found to correspond for all ILs to a nominal purity higher than 99%, apart form $[C_{10}C_1Im][Tf_2N]$ where a purity of higher than 98% was found. The water mass fractions of the samples were measured with Karl Fischer coulometric titration (Metrohm, 756 KF coulometer). The expanded uncertainty with a level of confidence of approximately 95% ($k = 2$) of the water content determinations performed within this work is estimated to be between ±20% and ±5%, corresponding to water mass fractions ranging from 5.0×10^{-5} to 1.0×10^{-2}. The halide contents were measured by titration with $AgNO_3$, and the obtained values were below the detection limit (<200 ppm).

$[C_8C_1Im]I$ was synthesized in the group of Dr. Pete Licence of the University of Nottingham and $[C_8C_1Im][NO_3]$ in the group of Prof. Stefan Spange of the University of Chemnitz; both ILs had a purity of >99%. $[C_4C_1Pyrr][Tf_2N]$ was kindly provided to us by Iolitec (www.iolitec.de, purity >99%) and $[C_8C_1Im][B(CN)_4]$ and $[C_8C_1Im][FAP]$ by Merck (purity >99%). $[C_2C_1Im][BF_4]$ and $[C_8C_1Im]Br$ were purchased from Merck with a purity of >98%. $[C_8C_1Im][BF_4]$, $[C_8C_1Im][PF_6]$, and $[C_8C_1Im][TfO]$ were purchased from Sigma-Aldrich with a purity of >97%, > 95%, and >97%, respectively. All purchased and donated ILs were used as obtained without further purification.

The nominal purity, water content, and halide content of the ILs studied in this work are summarized in Table 2. All parts of the measuring devices which were in contact with the sample as well as glassware used for sample handling were cleaned, rinsed with double-distilled water, and oven-dried. In order to avoid any surface-active impurity, we have experienced in our laboratories that extreme care should be taken to keep glassware for the preparation of "surface clean" ILs strictly separated from cleaning baths and washing solutions used for the purification of the ordinary laboratory glassware in order to avoid Si-surface contaminations of the sample ILs by traces of laboratory grease.

Angle-Resolved X-ray Photoelectron Spectroscopy (ARXPS). To ensure that the IL surfaces were free of surface active contaminants like polysiloxanes[42] and oxygen-containing carbohydrates,[43] all ILs were characterized with angle-resolved X-ray photoelectron spectroscopy (ARXPS) prior to the surface tension measurements. Furthermore, ARXPS was used to make a statement about the orientation of the ions at the IL/air interface. For experimental details see ref 44.

TABLE 1: Summary of ILs Investigated in This Study

Chemical Formula	Structure	Name
$[C_nC_1Im][Tf_2N]$ (n = 1, 2, 4, 6, 8, 10, 12)	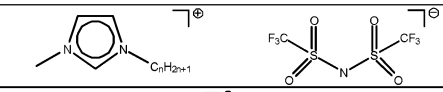	1-alkyl-3-methylimidazolium bis[(trifluoromethyl)sulfonyl]imide
$[Me(EG)_2C_1Im][Tf_2N]$	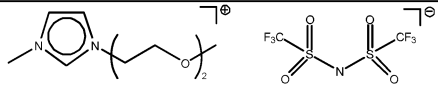	1-[2-(2-methoxy-ethoxy)ethyl]-3-methylimidazolium bis[(trifluoromethyl)sulfonyl]imide
$[C_4C_1Pyrr][Tf_2N]$	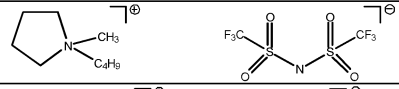	1-butyl-1-methylpyrrolidinium bis[(trifluoromethyl)sulfonyl]imide
$[C_2C_1Im][BF_4]$	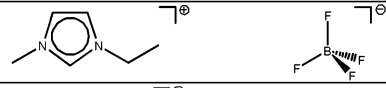	1-ethyl-3-methylimidazolium tetrafluoroborate
$[C_8C_1Im]Cl$	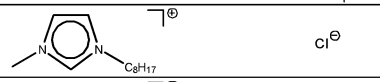	1-methyl-3-octylimidazolium chloride
$[C_8C_1Im]Br$		1-methyl-3-octylimidazolium bromide
$[C_8C_1Im]I$		1-methyl-3octylimidazolium iodide
$[C_8C_1Im][NO_3]$	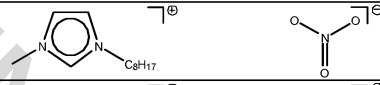	1-methyl-3-octyl-imidazolium nitrate
$[C_8C_1Im][BF_4]$	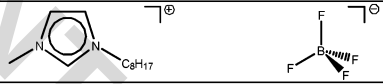	1-methyl-3-octylimidazolium tetrafluoroborate
$[C_8C_1Im][PF_6]$		1-methyl-3-octylimidazolium hexafluorophosphate
$[C_8C_1Im][B(CN)_4]$		1-methyl-3-octylimidazolium tetracyanoborate
$[C_8C_1Im][MeOSO_3]$	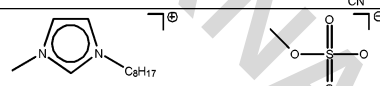	1-metyl-3-octylimidazolium methylsulfate
$[C_8C_1Im][TfO]$	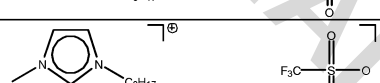	1-methyl-3-octylimidazolium trifluoromethylsulfonate
$[C_8C_1Im][Pf_2N]$	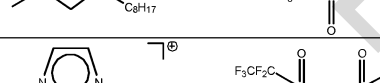	1-methyl-3-octylimidazolium bis[(pentafluoroethyl)sulfonyl]imide
$[C_8C_1Im][FAP]$	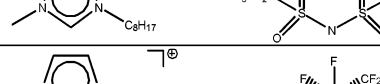	1-methyl-3-octylimidazolium tris(pentafluoroethyl)trifluorophosphate

Density Measurements: Vibrating Tube Method. Mass density measurements at atmospheric pressure were based on the vibrating tube method. For the density meter (Anton Paar, DMA 5000) used here, long-term drift is eliminated by a reference oscillator built into the measuring cell and only one adjustment at 293.15 K is sufficient to reach a high accuracy for the whole measuring temperature range. The DMA 5000 allowed for a full-range viscosity correction, whereby all viscosity-related errors inherent to all known types of oscillating U-tube density meters were automatically eliminated (information given by the supplier company). The temperature of the U-tube was controlled within ±1 mK and measured by a high-precision platinum resistance probe with an uncertainty of ±10 mK (values provided by supplier). For the density meter calibration, deionized water and dry air were measured as standards for each individual IL density measurement. In addition, the calibration of the density meter was frequently checked by measuring the liquid density of toluene at atmospheric pressure for temperatures between 278.15 and 343.15 K. The differences to literature values[45] were smaller than 0.01%. The expanded uncertainty at a 95% confidence level (k = 2) of the present density measurements for ILs was thus estimated to be less than ±0.02% taking the calibration uncertainty of the apparatus of 0.01% and the uncertainty associated with the measurement procedure for ILs into account. (Note that the precision or repeatability of the instrument was better than ±0.001%.)

As the quantities of $[C_8C_1Im]Cl$ and $[C_8C_1Im][TfO]$ were insufficient for the vibrating tube method (at least, 1 mL required), the densities of these two ILs were measured at 25 °C by weighing a defined volume of the IL (at least 0.100 mL) with an analytical balance (with a precision of ±0.1 mg). With this method, a relative uncertainty in density $d\rho/\rho$ values below 1.5% was achieved.

Surface Tension Measurements: Pendant Drop Technique. Surface (or better, interfacial[16]) tensions at the ionic liquid/gas interface were obtained by the pendant drop method. Here, a

TABLE 2: Molar Mass M, Nominal Purity, Concentration of Water and Halide by Mass w_{water} and w_{halide}, Density ρ, Molecular Volume V_m, Thermal Expansion Coefficient α_p, and Surface Tension σ at 298.15 K for All the Investigated ILs

ionic liquid	M/g mol^{-1}	purity/%	w_{water}/ppm	w_{halide}/ppm	ρ^b/g cm^{-3}	V_m/nm^3	$\alpha_p/10^{-4}$ K^{-1}	σ/mN m^{-1}
$[C_1C_1Im][Tf_2N]$	377.29	>99	77	na	1.567	0.400	7.43	36.3
$[C_2C_1Im][Tf_2N]$	391.31	>99[a]	509[a]	na	1.518[a]	0.428[a]	6.65	35.1[a]
$[C_4C_1Im][Tf_2N]$	419.37	>99	69	<200	1.435	0.485	6.66	30.7
$[C_6C_1Im][Tf_2N]$	447.42	>99	80	<200	1.364	0.545	6.89	30.2
$[C_8C_1Im][Tf_2N]$	475.47	>99	78	<200	1.311	0.603	6.75	29.5
$[C_{10}C_1Im][Tf_2N]$	503.53	>98	91	<200	1.270	0.659	6.78	29.5
$[C_{12}C_1Im][Tf_2N]$	531.58	>99	49	<200	1.244	0.710	6.80	29.8
$[C_4C_1Pyrr][Tf_2N]$	422.41	>99	<100	<200	1.394	0.503	6.32	32.3
$[Me(EG)_2C_1Im][Tf_2N]$	465.39	>99	<300	na	1.455	0.531	6.78	36.5
$[C_2C_1Im][BF_4]$	197.97	>98	<10000	<1000	1.280	0.257	5.95	53.9
$[C_8C_1Im]Cl$	230.78	>99	na	–	1.009	0.380	–	30.9
$[C_8C_1Im]Br$	275.23	>98	<10000	–	1.169	0.390	5.85	31.6
$[C_8C_1Im]I$	322.23	>99	na	–	1.305	0.410	5.90	32.7
$[C_8C_1Im][NO_3]$	257.33	>99	na	na	1.065	0.401	5.88	33.3
$[C_8C_1Im][BF_4]$	282.13	>97	na	na	1.099	0.426	6.18	30.8
$[C_8C_1Im][PF_6]$	340.29	>95	<500	na	1.235	0.458	6.27	32.5
$[C_8C_1Im][B(CN)_4]$	310.21	>99	59	<37	0.975	0.528	7.19	38.6
$[C_8C_1Im][MeOSO_3]$	306.42	>99	115	na	1.110	0.459	5.88	30.1
$[C_8C_1Im][TfO]$	344.40	>97	4780	na	1.142	0.501	–	28.5
$[C_8C_1Im][Pf_2N]$	575.49	>99	30	<200	1.396	0.685	7.02	27.7
$[C_8C_1Im][FAP]$	640.34	>99	49	<40	1.497	0.711	6.96	30.3

[a] Reference 31. [b] Calculated out of $\rho-T$-polynomial fit.

universal surface analyzer (OEG, SURFTENS universal) was used, where the geometrical profile of a pendant drop is compared with the theoretical drop profile obtained from the Laplace equation. The measurements were performed inside an optical glass cell for photometry (Hellma, 402.000) at room temperature, which was in the range of 292.9−298.5 K under ambient conditions. For the surface tension data of all ILs, the expanded uncertainty at the 95% confidence level ($k = 2$) was estimated to be less than ±1%.

3. Results and Discussion

In Table 2 the molecular weight (M), density (ρ), molecular volume (V_m) ($V_m = (M/\rho)/N_A$; N_A is Avogadro's constant), thermal expansion coefficient (α_p), and the surface tension (σ) are listed for all investigated ILs for a temperature of 25 °C (298.15 K); values for 20 °C (293.15 K) are provided in Table S2 in the Supporting Information. In the following, the effect of the cation and the anion on the density and surface tension will be discussed.

3.1. Density. The results of the density measurements in the temperature range from 278 to 308 K are summarized in Figure 1, a and b, for the $[Tf_2N]^-$ and the $[C_8C_1Im]^+$ salts, respectively (see also Table S1 in the Supporting Information). As expected, for every measured IL the density decreases with increasing temperature. The $\rho-T$ dependency of ILs can be well described with a polynomial of second order[31]

$$\rho = \rho_0 + \rho_1 T + \rho_2 T^2 \quad (1)$$

where T is the temperature in Kelvin and ρ_0, ρ_1, and ρ_2 are the fit parameters given in Table 3. For each IL the obtained standard percentage deviations are below the measurement uncertainty of ±0.02%; only for $[C_1C_1Im][Tf_2N]$ a higher deviation of 0.11% was found. For this IL, the density measurements were performed close to the melting point of $[C_1C_1Im][Tf_2N]$, which Tokuda et al. determined to be at 26 °C.[46] Hence, only density data in the temperature range from 293 K (where the IL was still in a supercooled liquid state) to 308 K were used for the $\rho-T$ dependency.

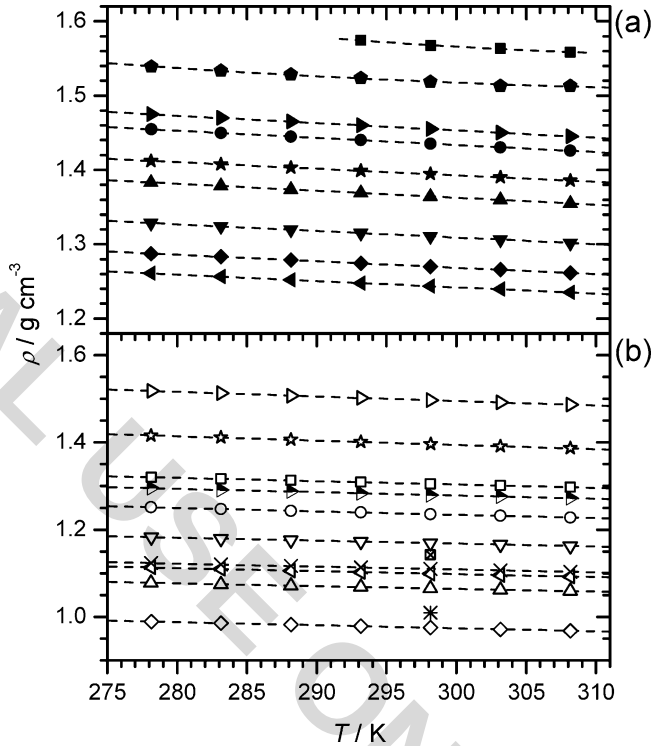

Figure 1. Density ρ as a function of temperature T of (a) the different $[Tf_2N]^-$ salts and (b) the different $[C_8C_1Im]^+$ salts: (■) $[C_1C_1Im][Tf_2N]$, (pentagon solid) $[C_2C_1Im][Tf_2N]$ (ref 31), (●) $[C_4C_1Im][Tf_2N]$, (▲) $[C_6C_1Im][Tf_2N]$, (▼) $[C_8C_1Im][Tf_2N]$, (♦) $[C_{10}C_1Im][Tf_2N]$, (left-pointing solid triangle) $[C_{12}C_1Im][Tf_2N]$, (★) $[C_4C_1Pyrr][Tf_2N]$, (right-pointing solid triangle) $[Me(EG)_2C_1Im][Tf_2N]$, (right-pointing open triangle) $[C_8C_1Im][FAP]$, (☆) $[C_8C_1Im][Pf_2N]$, (□) $[C_8C_1Im]I$, (○) $[C_8C_1Im][PF_6]$, (▽) $[C_8C_1Im]Br$, (crossed square) $[C_8C_1Im][TfO]$, (×) $[C_8C_1Im][MeOSO_3]$, (left-pointing open triangle) $[C_8C_1Im][BF_4]$, (△) $[C_8C_1Im][NO_3]$, (∗) $[C_8C_1Im]Cl$, (◇) $[C_8C_1Im][B(CN)_4]$, (right-pointing, half-filled triangle) $[C_2C_1Im][BF_4]$.

From the temperature-dependent density data the thermal expansion coefficient, α_p, can be calculated by

TABLE 3: Fit Parameters for Density ($\rho = \rho_0 + \rho_1 T + \rho_2 T^2$)

cation	anion	ρ_0/g cm^{-3}	$\rho_1/10^{-3}$ g cm^{-3} K^{-1}	$\rho_2/10^{-6}$ g cm^{-3} K^{-2}	rms[a]
$[C_1C_1Im]^+$	$[Tf_2N]^-$	4.0296	−15.3559	23.8000	0.1140
$[C_2C_1Im]^+$	$[Tf_2N]^-$	1.8506[b]	−1.2178[b]	0.3477[b]	0.0005[b]
$[C_4C_1Im]^+$	$[Tf_2N]^-$	1.7457	−1.1264	0.2868	0.0058
$[C_6C_1Im]^+$	$[Tf_2N]^-$	1.6596	−1.0403	0.1686	0.0009
$[C_8C_1Im]^+$	$[Tf_2N]^-$	1.6046	−1.0864	0.3381	0.0037
$[C_{10}C_1Im]^+$	$[Tf_2N]^-$	1.5894	−1.2812	0.7045	0.0037
$[C_{12}C_1Im]^+$	$[Tf_2N]^-$	1.5813	−1.4203	0.9647	0.0023
$[C_4C_1Pyrr]^+$	$[Tf_2N]^-$	1.6892	−1.0969	0.3623	0.0030
$[Me(EG)_2C_1Im]^+$	$[Tf_2N]^-$	1.7678	−1.1118	0.2102	0.0010
$[C_2C_1Im]^+$	$[BF_4]^-$	1.5372	−0.9667	0.3448	0.0009
$[C_8C_1Im]^+$	Br^-	1.3246	−0.3580	−0.5459	0.0031
$[C_8C_1Im]^+$	I^-	1.5148	−0.6377	−0.2222	0.0102
$[C_8C_1Im]^+$	$[NO_3]^-$	1.3776	−1.4703	1.4154	0.0095
$[C_8C_1Im]^+$	$[BF_4]^-$	1.3739	−1.1629	0.8106	0.0111
$[C_8C_1Im]^+$	$[PF_6]^-$	1.5843	−1.5665	1.3286	0.0074
$[C_8C_1Im]^+$	$[B(CN)_4]^-$	1.2058	−0.8472	0.2453	0.0015
$[C_8C_1Im]^+$	$[MeOSO_3]^-$	1.3600	−1.0247	0.6234	0.0066
$[C_8C_1Im]^+$	$[Pf_2N]^-$	1.7592	−1.4565	0.7996	0.0047
$[C_8C_1Im]^+$	$[FAP]^-$	1.8971	−1.6426	1.0069	0.0038

[a] Standard percentage deviation of ρ to the fit. [b] Reference 31.

$$\alpha_p = -\left(\frac{\partial \ln \rho}{\partial T}\right)_p \quad (2)$$

where p is the pressure. The resulting thermal expansion coefficients at 298.15 K are also given in Table 2. The calculated values lie in a range of (5.85−7.43) × 10^{-4} K^{-1}, which are typical values for ILs.[47,48] With the exception of $[C_8C_1Im]Br$ and $[C_8C_1Im]I$, where a weak increase of the thermal expansion coefficient α_p with increasing temperature was deduced, for all other ILs weakly decreasing values of α_p with increasing temperature were measured. A comparison of our data for $[C_2C_1Im][BF_4]$ and $[C_8C_1Im][BF_4]$ shows good agreement with data given by Troncoso et al., who attributed negative values for $(\partial\alpha/\partial T)_p$ to the high degree of cohesion in these systems.[49]

Effect of the Cation. In the following, the influence of the cation on the density, ρ, of the $[Tf_2N]^-$ salts will be discussed. In particular, three different aspects will be addressed: (i) the length of the alkyl chain on the imidazolium, (ii) the functionalization of the chain with hydrophilic groups, and (iii) the head group of the cation.

The influence of the alkyl chain length on the density was studied for $[C_nC_1Im][Tf_2N]$, with n = 1, 2, 4, 6, 8, 10, 12. As evident from Table 2, the density of these ILs decreases with increasing alkyl chain length, from 1.567 g cm^{-3} for $[C_1C_1Im][Tf_2N]$ to 1.244 g cm^{-3} for $[C_{12}C_1Im][Tf_2N]$. This trend was seen before, independent of the anion and of the cationic head group.[1,18,50,51] Moreover, the same behavior was observed for alkyl chains covalently bonded on the anion.[26,27] Similar effects were also found for molecular liquids with polar groups like esters and alkyl carbonates.[52] Interestingly, the opposite trend is found for linear alkanes and primary alcohols, where the density *increases* with increasing alkyl chain length.[53] For these cases, increasing dispersive interactions between the aliphatic carbon chains with increasing chain length leads to a denser packing. In ILs the dispersive interactions also increase with chain length, resulting in a nanostructural organization (separation) in polar and nonpolar regions (domains).[54,55] The nonpolar regions are made up of alkyl groups whereas the polar ones contain the cationic head groups and the anions. By increasing the chain length, the nonpolar regions increase and take up more and more space, resulting in a lower overall density. In contrast to alkanes or alcohols, however, the packing of the chains within the nonpolar domains of ILs is limited simply by the existence of the polar regions (due to charged head groups covalently attached to the chains). Our data in Figure 2 reveal a linear increase of the molecular volume V_m with increasing alkyl chain length and hence an ideal behavior. From the slope of the linear fit to dV_m/dn, with n being the chain length of $[C_nC_1Im][Tf_2N]$, the molecular volume of one methylene group (−CH$_2$−) is calculated to be 0.0283 nm^3 at 298.15 K, corresponding to a molar volume of 17.0 cm^3 mol^{-1}. These values agree well with the calculations of Glasser et al. (0.0282 nm^3) and Tariq et al. (17 cm^3 mol^{-1}).[47,56] From the intersection with the y-axis at n = 0, a molecular volume for the $[-C_1Im]^+[Tf_2N]^-$ ionic head group of 0.371 nm^3 is deduced.

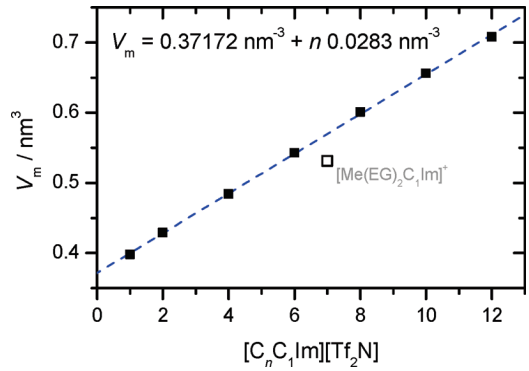

Figure 2. Dependence of the IL molecular volume V_m at 298.15 K on the chain length of the $[C_nC_1Im][Tf_2N]$ series. Moreover, the molecular volume of $[Me(EG)_2C_1Im][Tf_2N]$ with its corresponding chain length of n = 7 atoms is also given for comparison (open square; for details, see text).

An interesting aspect is the introduction of hydrophilic ethylene glycol groups into the alkyl chain. $[Me(EG)_2C_1Im][Tf_2N]$ has two oxygen and five carbon atoms in its functionalized side chain. Thus, one could naively expect a density similar to that of $[C_7C_1Im][Tf_2N]$. However, the introduction of the ethylene glycol groups leads to a significantly increased density, as can be seen by comparing the values of 1.455 g cm^{-3} for $[Me(EG)_2C_1Im][Tf_2N]$ and 1.337 g cm^{-3} for the nonfunctionalized IL (estimated as average value for $[C_6C_1Im][Tf_2N]$ and $[C_8C_1Im][Tf_2N]$; see Table 2). The resulting difference of ∼9% is much larger than to be expected just from the smaller volume of the O atom as compared to the −CH$_2$− group and from the difference in molar mass (also note that the

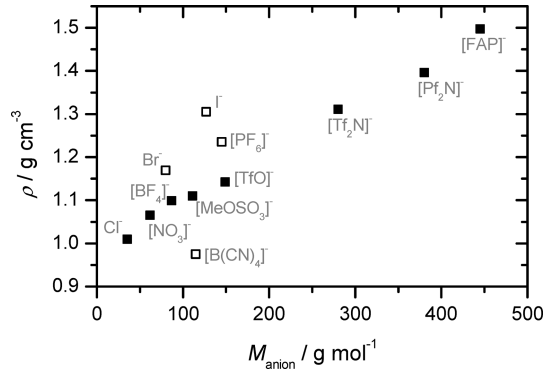

Figure 3. Density ρ of the $[C_8C_1Im]X$ ILs as a function of molar mass of the anion M_{anion} at 298.15 K.

difference in ρ for $[C_6C_1Im][Tf_2N]$ vs $[C_8C_1Im][Tf_2N]$) is only 4%). This trend is consistent with results from the literature: Himmler et al. found a higher density for $[C_2C_1Im][Me(EG)_2OSO_3]$ than for the corresponding $[C_2C_1Im][C_8H_{17}OSO_3]$ homologue.[57] Similar trends were observed in non-IL systems such as ethylene glycol-functionalized hydrocarbons, which exhibit a higher density than their nonfunctionalized homologues.[58] The higher density of the functionalized systems is therefore attributed to the formation of inter- and intramolecular H-bonds. In particular for ILs, the formation of H-bonds between the ether groups and the acidic hydrogen atoms of the imidazolium ring results in a denser packing than for the nonfunctionalized IL.[59,60] This deviation from ideal packing behavior is also evident from Figure 2, where the molecular volume of $[Me(EG)_2C_1Im][Tf_2N]$ (open square symbol) lies considerably below that expected for $[C_7C_1Im][Tf_2N]$.

Changing the head group of the cation from imidazolium to pyrrolidinium decreases the density as can be seen by comparing the values of $\rho = 1.435$ g cm^{-3} for $[C_4C_1Im][Tf_2N]$ and 1.394 g cm^{-3} for $[C_4C_1Pyrr][Tf_2N]$ in Table 2. The data of Tokuda et al. and Jin et al. confirm this trend for the same ILs.[46,61] It is believed that due to the planar configuration of the imidazolium ring a denser packing can be achieved than in the pyrrolidiniuim IL. However, Sanchez et al. observed the reverse trend (i.e., higher density for the pyrrolidinium IL) when using the dicyanamide anion.[51] They suggested that the anion influences the preferential conformation of the cation which should have an effect on the density. Further studies are necessary to confirm this suggestion.

Effect of the Anion. To study the influence of the anion on the density, various ILs with the same cation, namely $[C_8C_1Im]^+$, were measured (see Table 2). The observed density increases in the order $[B(CN)_4]^- < Cl^- < [NO_3]^- < [BF_4]^- < [MeOSO_3]^- < [TfO]^- < Br^- < [PF_6]^- < [Tf_2N]^- \approx I^- < [Pf_2N]^- < [FAP]^-$. As can be seen in Figure 3, the density generally increases with increasing molecular weight of the anion. Only the ILs containing Br^-, I^-, $[PF_6]^-$, and $[B(CN)_4]^-$ (open squares) do not really follow a more or less linear relationship. Considering the van der Waals radii, the bond lengths, and the atomic weight of the anions these findings are not unexpected. To illustrate this, a comparison of bromide and the approximately spherical $[BF_4]^-$ is made. Both anions have nearly the same molecular weight, but the radius of bromide is smaller than the radius of $[BF_4]^-$ leading to a denser packing of $[C_8C_1Im]Br$ as it is also witnessed by their molecular volume of 0.426 and 0.390 nm^3, respectively.

Effect of Water Content. In comparison to other thermophysical properties of ILs, e.g., viscosity, the influence of the water content on the density is very small due to the large differences in molecular weights (190−640 g/mol vs 18 g/mol)

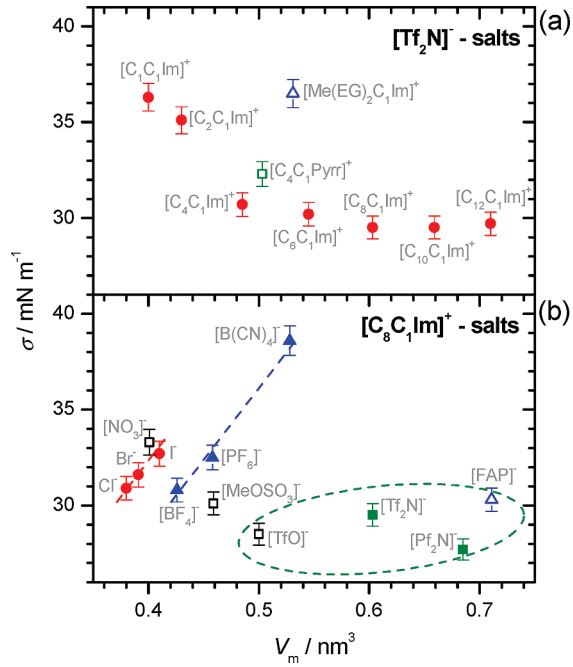

Figure 4. Surface tension σ of (a) $[Tf_2N]^-$ salts and (b) $[C_8C_1Im]^+$ salts at $T = 298.15$ K as a function of IL molecular volume V_m. Dashed lines indicate trends in subgroups discussed in the text.

and the minor differences in densities (1.0−1.6 g/cm^{-3} vs 1.0 g/cm^{-3}) of the ILs and of water, respectively. In a first approximation, the change in density of ILs with water contents up to several weight percent of water in ILs follows an ideal behavior as it was investigated for several IL−water mixtures by us and by other groups.[62,63] Even a water content of, e.g., 10 wt % (i.e., about 10 times higher than the largest value given in Table 2) would decrease the density of $[C_4C_1Im][BF_4]$ only from 1.28 to 1.25 g/cm^3 which is in the order of the size of the data points of Figures 1 and 3 and, thus, our discussion on IL densities is not affected by residual water.

3.2. Surface Tension. All surface tension (ST) values, σ, were obtained at room temperature ($292.9 < T < 298.5$ K) and at atmospheric pressure. From these values and the temperature dependency of the density, the ST was calculated for a temperature of 298.15 K by[64,65]

$$\sigma_{25°C} = \sigma_{RT}(\rho_{25°C}/\rho_{RT})^4 \quad (3)$$

where σ_{RT} and ρ_{RT} are the measured ST and density at room temperature. This approach yields values for the ST at a given temperature of highly viscous fluids typically with an uncertainty of less than 2%, as was tested for several reference fluids, see, e.g., ref 66.

The ST values corrected to 25 °C are summarized in Table 2 (for comparison with literature, ST values for 20 °C are also provided in Table S2 in the Supporting Information). To allow for a visual comparison, the ST is plotted as a function of ionic liquid molecular volume in Figure 4, a and b, for the $[Tf_2N]^-$ and the $[C_8C_1Im]^+$ salts, respectively, on the same scales. A detailed discussion on the influence of the chemical nature of cation and anion will follow in the next paragraphs. In addition to Figure 4, we have plotted our data along with all available literature data in Figure 5, a and b, for the $[Tf_2N]^-$ and the $[C_8C_1Im]^+$ salts, respectively. The deviations of the literature data from our data lie between −13% and +22%, with the

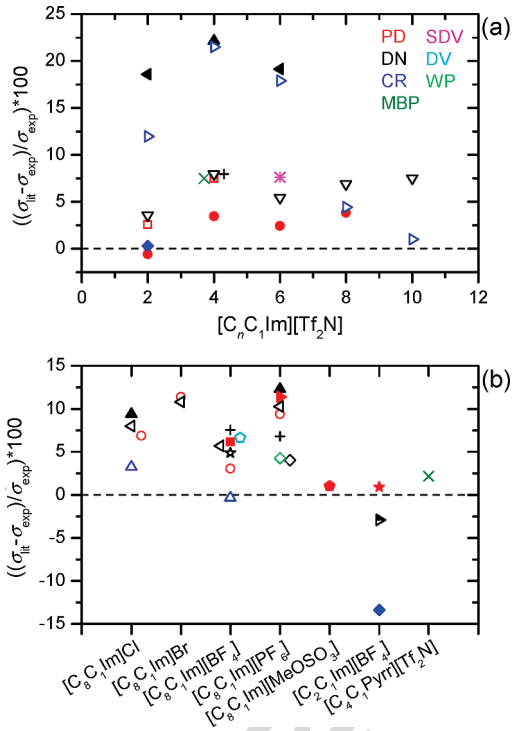

Figure 5. Percent deviation between the surface tension data of this work σ_{exp} (at 298.15 K) and ST values from other groups (σ_{lit}); σ_{lit} values provided for other temperatures (values in parentheses) were extrapolated to 298.15 K using eq 3: (□) ref 48, (●) ref 20, (◆) ref 33 (295.15−298.15 K), (▲) ref 93, (▽) ref 19 (293.15 K), (left-pointing solid triangle) ref 94, (right-pointing open triangle) ref 18, (+) ref 22 (293.15 K), (×) ref 61, (∗) ref 85, (○) ref 95 (313.15 K) [surface tension of $[C_8C_1Im]Cl$ was extrapolated to the given temperature by using the $\rho-T$ dependency of $[C_8C_1Im]Br$], (◇) ref 96 (303.15 K), (■) ref 97, (left-pointing open triangle) ref 32 (336.15 K) [surface tension of $[C_8C_1Im]Cl$ was extrapolated to the given temperature by using the $\rho-T$ dependency of $[C_8C_1Im]Br$], (right-pointing solid triangle) ref 50, (⬠) ref 67, (△) ref 24, (solid pentagon) ref 27, (☆) ref 51, (★) ref 26, (right-pointing half-filled triangle) ref 98 (293.15 K). Color code: red = pendant drop (PD), black = du Noüy ring (DN), blue = capillary rise method (CR), olive = maximum bubble pressure (MBP), magenta = spinning drop video (SDV), cyan = drop volume tensiometer (DV), green = Wilhelmy plate (WP).

maximum deviation found for $[C_4C_1Im][Tf_2N]$. For $[Me(EG)_2C_1Im][Tf_2N]$ and $[C_8C_1Im]X$ (where X = I^-, $[NO_3]^-$, $[B(CN)_4]^-$, $[TfO]^-$, $[Pf_2N]^-$, and $[FAP]^-$), to the best of our knowledge, no reported data are available yet. In most cases, our ST values measured for the different ILs are smaller than observed in the other studies. Deviations larger than ±10% most often occur for ST values obtained by the du Noüy ring and the capillary rise method (black and dark blue symbols in Figure 5) which might point toward systematic deviations depending on the experimental method. In comparison to the ring method, the pendant drop method is based on rigid working equations, where no calibration procedure or correction is needed and the reliability of the measurements can be easily checked (see also the discussion on various ST methods in ref 35).

Another possible reason for deviations in the ST values found in different studies could be related to additional contaminations of the ILs, e.g., a different water content. However, recent studies indicate that water as one of the most likely IL contaminations has a minor effect only; e.g., 26 mol % of water in $[C_8C_1Im]Br$ increases the ST only about +0.3% in comparison to neat $[C_8C_1Im]Br$. A similar behavior was found for the binary mixtures of water and $[C_nC_1Im][BF_4]$ (n = 2, 4, 6),[67−70] $[C_nC_1Im]Cl$ (n = 10, 12),[71] or $[C_2C_1Im][EtOSO_3]$,[72] which shows that the ST is approximately constant in the IL-rich phase with only slight increase of the ST with water content. This observation can be explained by the work of Rivera-Rubero et al., who measured the surface of the water/$[C_4C_1Im][BF_4]$ mixture with sum frequency generation spectroscopy (SFG).[73] They found that, at a mole fraction χ_{IL} greater than 0.02, the surface of the mixture is only made up of the IL and the orientation of the ions at the IL surface is not influenced by water. Apart from bulk water in equilibrium with the gas phase, an influence of the vapor pressure of water in the atmosphere above IL surfaces is reported for the ST (more precisely, interface tension) of hygroscopic and hydrophobic ILs. In these cases, transient adsorption of water molecules in the near-surface region seems to occur.[74,75] This adsorption generally leads to a moderate decrease of the ST, as was shown by Freire et al.[22] The atmospheric saturation of $[C_8C_1Im][PF_6]$ with water decreases the ST by 0.6% and for the more hydrophilic $[C_8C_1Im][BF_4]$ by 2%. The authors explain this decrease of ST with the reduction of electrostatic attractions between the ions due to the formation of hydrogen bonds between water and the anions and cations in the near-surface region. Baldelli supports this explanation within a sum frequency generation (SFG) study for $[C_4C_1Im][Tf_2N]$ and $[C_4C_1Im][PF_6]$.[76] He also showed that at water pressures greater than 5×10^{-4} Torr reorientation effects of IL ions at the surface occur due to embedded water molecules in the near-surface region. In any case, the presence or absence of surface water cannot solely explain the large deviations in ST values of several tens of percents in the different studies.

Previous investigations of IL surfaces by X-ray induced photoelectron spectroscopy (XPS) showed that there is the possibility of nonvolatile, surface-active contaminations like oxygen-containing carbohydrates and polysiloxanes,[42,43,77] which should have an effect on the ST. The main origin of these contaminants is expected to be the IL synthesis process where the IL often gets in contact with lubricating grease that is commonly used in synthetic laboratories for the sealing of glass fittings. Even a minor contamination concentration in the bulk IL can lead to a surface completely covered with a contamination layer if surface enrichment effects take place.[42] As emphasized in the Experimental Section, the absence of surface active contaminants in our ST studies was verified by characterizing each IL with surface-sensitive ARXPS before (and in selective cases also after) ST measurements.

Effect of the Cation. *(a) Alkyl Chains.* The ST of the $[C_nC_1Im][Tf_2N]$ series is plotted in Figure 4a as a function of IL molecular volume (square symbols). For the short alkyl chains ($n \leq 8$), the ST strongly decreases with increasing alkyl chain. For imidazolium-based ionic liquids this trend was observed before by various groups; some of them measured the same $[C_nC_1Im][Tf_2N]$ system,[18−21] others used a different anion,[17,22−24] and a few concentrated on ILs where the alkyl chain is attached to the anion.[25−27] Zhou et al. attributed this behavior to a weakening of the Coulomb interaction when increasing the alkyl chain length.[26] However, molecular dynamics simulation by Ludwig et al., who calculated the Coulomb and Lennard-Jones (van der Waals interaction) energies of $[C_nC_1Im][Tf_2N]$ (n = 1, 2, 4, 6, 8), show that the Coulomb interaction in the bulk is only very weakly influenced by the alkyl chain length if $n \geq 2$; only $[C_1C_1Im][Tf_2N]$ exhibits a higher value for the Coulomb energy due to the symmetry of the cation. In contrast, the van der Waals interactions are clearly dependent on the alkyl chain length. The longer the alkyl chain, the stronger the attractive Lennard-Jones contribution.[78] Ac-

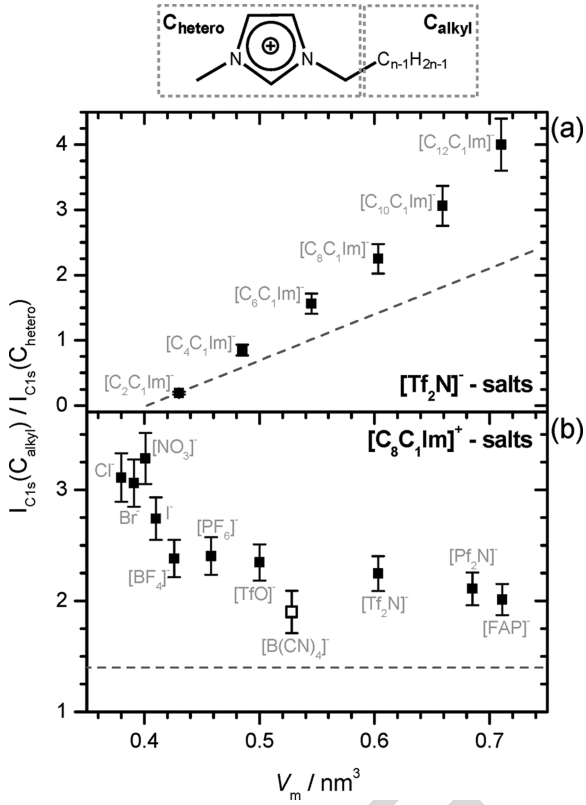

Figure 6. Ratio of the XPS peak intensities measured in 80° (most surface sensitive) of the cations chain atoms (C_{alkyl}) vs the five carbon atoms of the imidazolium head group (C_{hetero}) as a function of IL molecular volume V_m for (a) $[C_nC_1Im][Tf_2N]$ and (b) $[C_8C_1Im]X$. (Dashed lines indicate nominal values for C_{alkyl} vs C_{hetero} as expected from IL stoichiometry, for details, see text).

cording to Langmuir's principle, only the parts of the molecule at the outer surface will mainly contribute to the ST.[36,37] A random orientation of the ions at the surface would therefore lead to a higher ST for the longer alkyl chain due to the increased Lennard-Jones energy as it is especially the case for alkanes.[53] As we demonstrate by ARXPS of the $[C_nC_1Im][Tf_2N]$ systems, there is in fact a preferential orientation of the ions at the IL surface.[39,44] Figure 6a shows the ratio of the C 1s XPS-peak intensities of the cation carbon atoms, $I_{C1s}(C_{alkyl})/I_{C1s}(C_{hetero})$, measured at an electron emission angle of 80° with respect to the surface normal; C_{hetero} corresponds to carbon atoms bonded to nitrogen neighbors in the charged head group and C_{alkyl} to carbon atoms bonded only to carbon neighbors in the alkyl chain (see sketch at the top of Figure 6). At 80° emission angle only the topmost layer (1−1.5 nm) is probed enabling us to make a statement about the surface composition. For ions at the surface with no preferential orientation, the value of the ratio $I_{C1s}(C_{alkyl})/I_{C1s}(C_{hetero})$ would be the nominal value (indicated by the dashed line in Figure 6a). This is the case for $[C_2C_1Im][Tf_2N]$, but for all ILs with a longer chain the ratio is higher than the nominal value. Therefore, C_{alkyl} (i.e., the alkyl chain) is unambiguously overrepresented at the surface and the following surface model can be drawn: the alkyl chains are sticking out toward the gas phase, forming an aliphatic overlayer above an ionic sublayer, which consists of the imidazolium rings and the $[Tf_2N]^-$ anions. With increasing alkyl chain length this effect gets more pronounced. The observed orientation of the cations with the alkyl chains at the outer surface was also confirmed by other groups using surface-sensitive methods like ARXPS,[79] SFG,[80,81] Rutherford backscattering,[77,82] or neutron reflectometry[83] as well as simulations.[28,29] In line with Langmuir's principle, the contribution of the aliphatic chains to the measured surface tension becomes more and more dominating with increasing chain length. Under the reasonable assumption that the dispersive interactions between the aliphatic chains (and, thus, their molecular ST contributions) are smaller than the Coulomb interactions between the charged head groups, the initial decrease of ST with increasing chain length (from $n = 2$ to 8) can be explained.

Increasing the chain length further from $[C_8C_1Im][Tf_2N]$ to $[C_{12}C_1Im][Tf_2N]$ does not have any further effect on the ST. The same behavior was observed by Carvalho et al. who also examined the $[C_nC_1Im][Tf_2N]$ series.[19] $[C_nC_1Im][C_mH_{2m+1}SO_4]$ salts ($n = 1, 2, 4, 6, 8$, $m = 1, 2$) show saturation of the ST at about 30 mN m^{-1} at a chain length of $n = 8$;[27] this ST value fits very well with our data of $[C_8C_1Im]^+$-based ILs. Coarse-grain molecular dynamics simulations of Jiang et al. for $[C_nC_1Im]X$ further confirm a constant ST value for chains longer than $n = 10$.[28] As there are not many ST studies of ionic liquids with chains longer than $n = 8$ (due to the increasing viscosity for very long alkyl chains), it is not known whether this saturation behavior holds true for imidazolium-based ILs in general. Jiang et al. referred to the Langmuir principle and proposed that as the surface for $[C_nC_1Im]X$ with $n \geq 10$ is only made up of the alkyl chains. Only these alkyl chains contribute to the ST, whereas the polar groups have a strongly reduced influence on the ST.[28] Another suggestion is that by increasing the chain length from $n = 8$ to $n = 12$ the higher van der Waals interaction (which would lead to a higher ST) and the smaller contribution of the Coulomb interaction (which would lead to a smaller ST) could compensate each other and, therefore, no further changes in the ST are observed. Up to this point, there is no clear experimental evidence to favor one of the possible explanations.

(b) Functionalized Chains. Functionalizing the hydrophobic alkyl chain with hydrophilic ether groups leads to an increased ST, as can be seen by comparing $[Me(EG)_2C_1Im][Tf_2N]$ and $[C_6C_1Im][Tf_2N]$ ($\sigma = 36.5 \pm 0.7$ and 30.2 ± 0.6 mN m^{-1}, respectively). In contrast to the nonfunctionalized IL, an additional interaction contributes to the ST. This interaction is induced by the ether groups, which in the bulk can form inter- and intramolecular H-bonds with the hydrogen-bond donor atoms of the imidazolium ring.[59,60] Furthermore, the H-bonding leads to a surface with no preferential orientation of the cations or surface enrichment of the chains as was shown in a previous ARXPS study.[39,44] Therefore, the contribution of Coulomb interactions due to the presence of the ionic head groups at the surface is higher for the functionalized IL than for the nonfunctionalized IL. In our opinion, both effects are responsible for the increase in ST of ILs carrying polyethylene glycol functionalities in their side chains.

(c) Cationic Head Group. The dependence of the ST on the cationic head group is analyzed by the comparison of $[C_4C_1Im][Tf_2N]$ and $[C_4C_1Pyrr][Tf_2N]$. In contrast to Jin et al. who observed a ST of 33.0 mN m^{-1} for both ILs,[61] we find a higher ST for the pyrrolidinium IL than for the imidazolium IL ($\sigma = 32.3 \pm 0.7$ and 30.7 ± 0.6 mN m^{-1}, respectively). Sanchez et al., who measured the ST of $[C_4C_1Pyrr][SCN]$ vs $[C_4C_1Im][SCN]$ (49.8 ± 0.1 vs 45.9 ± 0.2 mN m^{-1} at 303.35 K) and $[C_4C_1Pyrr][N(CN)_2]$ vs $[C_4C_1Im][N(CN)_2]$ (55.8 ± 0.2 vs 48.6 ± 0.1 mN m^{-1} at 303.38 K),[51] support our trend that pyrrolidinium ILs have a higher ST than their imidazolium homologues. An explanation can be found in the work of Deyko et al.,[84] who measured the enthalpy of vaporization of a range of ILs at 298 K, which is intimately related to the different

interaction contributions in the bulk. The authors found that the Coulomb interactions for $[C_4C_1Pyrr][Tf_2N]$ and $[C_4C_1Im][Tf_2N]$ are nearly the same (74 and 75 kJ mol^{-1}, respectively) whereas the van der Waals interactions in the pyrrolidinium IL are stronger than in the imidazolium IL (79 and 59 kJ mol^{-1}, respectively),[84] which would be consistent with the larger ST observed for the pyrrolidinium IL.

As in the case of the functionalized ILs discussed above, surface orientation effects most likely contribute to the higher ST value of $[C_4C_1Pyrr][Tf_2N]$ compared to $[C_4C_1Im][Tf_2N]$, too. In ARXPS, both ILs exhibit changes of core level intensities that indicate that the butyl chains preferentially point toward the vacuum. However, the degree of orientation is different for the two ILs (see also Figure S1 in the Supporting Information). For $[C_4C_1Im][Tf_2N]$ both N 1s signals from the charged moieties (i.e., from the two nitrogen atoms of the imidazolium ring at 401.7 eV and the nitrogen atom of the $[Tf_2N]^-$ anion at 399.0 eV) decrease by about 20% when going from 0° emission angle (more bulk sensitive) to 80° (more surface sensitive). The decrease at 80° is mainly caused by signal attenuation of the cationic head group due to the aliphatic overlayer at the outermost surface (note that the same effect, namely the decrease in imidazolium ring carbon intensity C_{hetero} due to signal damping, mainly causes the increase in C_{alkyl}/C_{hetero} ratio above the nominal value in Figure 6). For $[C_4C_1Pyrr][Tf_2N]$, the N 1s signals of both cation (402.4 eV) and anion (399.1 eV) at 80° are only 10% smaller than at 0°, which clearly indicates a lower degree of orientation of surface cations as compared to its imidazolium analogue. It is tempting to speculate here that the different degree of alkyl chain enrichment is related to the more bulky $[C_4C_1Pyrr]^+$ cation with its sp^3-hybridized pyrrolidinium nitrogen as compared to the planar geometry of the imidazolium ring. Within the framework of Langmuir's principle, the different degree of surface order in both ILs (and, thus, the different compositions of the outer surfaces) should affect the ST values: apart from different attractive interactions in the bulk discussed at the beginning of this paragraph, the pyrrolidinium IL with the lower alkyl enrichment and therefore larger presence of the charged head groups at the outer surface also leads to an overall increase of the Coulomb contribution and, thus, to a higher ST as compared to the ST of $[C_4C_1Im][Tf_2N]$.

Effect of the Anion. To study the influence of the anion on the ST, 12 different ILs were chosen with the same cation ($[C_8C_1Im]^+$) and a variety of anions containing small (halides, $[NO_3]^-$, and $[BF_4]^-$), medium-sized ($[PF_6]^-$, $[B(CN)_4]^-$, $[MeOSO_3]^-$, and $[TfO]^-$), and large, weakly coordinating anions ($[Tf_2N]^-$, $[Pf_2N]^-$, and $[FAP]^-$). The ST as a function of molecular volume is plotted in Figure 4b. In the literature there are different statements concerning the dependence of the ST on the molar volume: with respect to the selected anions it is found that the ST either increases[32,85] or decreases[21,22] with increasing anion size, or that there is no dependence at all.[33,51] As can be seen in Figure 4b for the ionic liquids measured in this work, there is only a very weak, if any, overall decrease of the ST with increasing molecular volume of the anion (except for $[C_8C_1Im][B(CN)_4]$, which will be discussed in detail later).

To explain the different ST values, we have to consider the anion dependency on the interaction strength and on the orientation of the ions at the surface. Considering the interaction strength, the Coulomb contribution will decrease and the dispersive contribution will increase with increasing anion size. Information about the orientation of the ions at the IL/gas interface is once again obtained by an ARXPS study of the $[C_8C_1Im][X]$ system.[40,44] As can be seen in Figure 6b, the value of the ratio $I_{C1s}(C_{alkyl})/I_{C1s}(C_{hetero})$ at 80° emission angle is higher than the nominal value (dashed line) for every measured $[C_8C_1Im]^+$-based IL; i.e., the octyl chain of the imidazolium is always enriched at the surface. However, the ratio $I_{C1s}(C_{alkyl})/I_{C1s}(C_{hetero})$ and, therefore, the level of chain enrichment depends on the molecular volume (which is related to the coordination strength of the anion to the head group of the imidazolium cation[86]): as the size of the anion increases and thus the coordination strength between anion and cation decreases, the level of enrichment decreases.[40] Due to the preferential orientation of the octyl chain toward the gas phase, the surface contribution of the Coulomb interaction to the ST will generally be smaller than for ILs with shorter alkyl chains. This can be seen by comparing the ST of $[C_2C_1Im][BF_4]$, $[C_8C_1Im][BF_4]$, $[C_2C_1Im][Tf_2N]$, and $[C_8C_1Im][Tf_2N]$ in Table 2. The anion-induced difference in ST of the two $[C_2C_1Im]^+$ salts is 18.8 mN m^{-1} (53.9 ± 1.1 vs 35.1 ± 0.7 mN m^{-1}) whereas the difference of the $[C_8C_1Im]^+$ salts is only 1.3 mN m^{-1} (30.8 ± 0.6 vs 29.5 ± 0.6 mN m^{-1}).

As the anions used in this work strongly vary in different aspects like size, shape, basicity, and, thus, coordinating ability, a general explanation for the ST values across the whole range of anions is still not available yet. However, dividing our $[C_8C_1Im]X$ series into subgroups of anions of chemical similarity, systematic ST changes are observed within these groups and will be discussed qualitatively in the following.

(a) Halides (Cl^-, Br^-, I^-). For the $[C_8C_1Im]^+$ halide ILs, the ST increases more or less linearly with increasing molecular volume in the order $Cl^- < Br^- < I^-$ which is in general agreement with ST data from IL literature for imidazolium based ILs. From a simple consideration of interacting point charges (to simulate the Coulomb forces), an opposite trend for this subseries would be expected: as the size of the anion, i.e., V_m, increases, the mean distance r between the cation head group and halide anion increases too. Consequently the interionic Coulomb attraction decreases, which leads to a decrease of the ST with V_m. Obviously, compensation effect(s) to the ST from non-Coulombic contributions lead to the observed opposite trend. To find an explanation, a comparison to the hydrogen halides is made. For the latter, the ST also increases in the order HCl < HBr < HI.[53] The main intermolecular interactions in the case of hydrogen halides are dipole−dipole interactions and van der Waals forces.[87] As the size of the halide anion increases, its polarizability and, therefore, the van der Waals contribution of the anion also increases;[88−90] this rise in dispersive attraction even overcompensates the concomitant decrease in attractive dipole−dipole contributions for increasing halide size (i.e., due to the largest electronegativity of chlorine in this series, dipole−dipole attractions are strongest for HCl).[87] Overall, a stronger intermolecular interaction in the bulk and, thus, a higher ST can be found for HI compared to HCl. With respect to the halide ILs of our study, we believe that the same explanation holds true: the gain in attractive van der Waals contribution of the anion increasing from $[C_8C_1Im]Cl$ to $[C_8C_1Im]I$ leads to the observed ST behavior. Apart from bulk cohesive energy, surface order effects may also contribute to the increase of ST with increasing anion size according to Langmuir's principle. As is shown in Figure 6b, the surface orientation of the alkyl chains is most pronounced for $[C_8C_1Im]Cl$ and $[C_8C_1Im]Br$ ($C_{alky}/C_{hetero} \approx 3.1$) whereas it is considerably reduced for $[C_8C_1Im]I$ ($C_{alky}/C_{hetero} \approx 2.7$). This is a clear indication that the number of charged head groups at the surface and, thus, their Coulomb contributions to the ST, is considerably increased for $[C_8C_1Im]I$

compared to the smaller halide anions, and, thus, leads to an increase in ST.

(b) Spherical Anions of the Structure $[XL_{4/6}]^-$. The anions $[BF_4]^-$, $[PF_6]^-$, and $[B(CN)_4]^-$ are all more or less of spherical shape and will therefore be considered in one group. Similar to the halides, the ST increases with anion size, in the order $[BF_4]^- < [PF_6]^- < [B(CN)_4]^-$. Since to the best of our knowledge no ST data for $[B(CN)_4]^-$ containing ILs are available, a comparison with literature cannot be made yet. For $[BF_4]^-$ and $[PF_6]^-$ the same trend as found here, i.e., a higher ST for $[PF_6]^-$ than $[BF_4]^-$ ILs (with the same cation) is found in the literature. Since polarizability values are not yet available for all anions, we refrain from adapting the qualitative argument given for the halide series in the previous paragraph.[91] A qualitative explanation for the ST increase in this series could once again be derived from the work of Deyko et al., who calculated the Coulomb and the van der Waals contributions for $[C_8C_1Im][BF_4]$ and $[C_8C_1Im][PF_6]$. The authors showed that the Coulomb energies in the bulk are nearly the same for both ILs whereas the van der Waals contributions related to the different anions are considerably higher in the $[PF_6]^-$ IL (by 14 kJ mol^{-1}).[84] In addition to bulk cohesive energies, the anisotropic surface composition of these three ILs deduced from ARXPS in terms of orientation of the octyl chain of the cation is also expected to contribute to the high ST value of $[C_8C_1Im][B(CN)_4]$. The C_{alkyl}/C_{hetero} ratio of ≈1.9 in Figure 6 witnesses the lowest degree of octyl chain enrichment for $[C_8C_1Im][B(CN)_4]$ compared to all other $[C_8C_1Im]X$ ILs of this study, in particular, compared to the value of 2.4 for $[C_8C_1Im][BF_4]$ and $[C_8C_1Im][PF_6]$. This implies a comparably larger presence of charged head groups of $[C_8C_1Im][B(CN)_4]$ at the surface, which results in an enhanced Coulomb contribution to the ST and thus could explain the higher ST values compared to $[C_8C_1Im][BF_4]$ and $[C_8C_1Im][PF_6]$.

(c) Perfluorinated Anions. The STs of the $[C_8C_1Im]^+$ ILs with fluoroalkyl-containing anions ($[TfO]^-$, $[Tf_2N]^-$, $[Pf_2N]^-$, and $[FAP]^-$) are all found in the lower range of the measured ST values (green oval in Figure 4b), i.e., between 27.7 and 30.3 mN m^{-1}. Higher values for the ST for linear or branched alkanes than for their perfluorinated homologues have been also observed in the literature.[92] The small ST of the latter is attributed to the very rigid and noncoordinating C−F bonds (in contrast to the polarizable C−H bonds in the case of hydrocarbons) leading only to weak attractive interactions between the CF_x groups; moreover, steric repulsion effects between CF_x groups are also proposed to be involved in lowering ST.[92] Adapting the analogy from perfluorated organic solvents, the four perfluorinated anions will be also compared with anions of our series which exhibit to some extend a similar configuration, namely $[MeOSO_3]^-$ with $[TfO]^-$ (both asymmetric anions, exchange of H_3C-O group by F_3C group in $[TfO]^-$), $[Tf_2N]^-$ with $[Pf_2N]^-$ (similar $-SO_2-N-SO_2-$ core, extended fluoroalkyl groups in the $[Pf_2N]^-$ ion), and $[PF_6]^-$ with $[FAP]^-$ (PL_6^- structure, three F ligands replaced by $-CF_2-CF_3$ groups in $[FAP]^-$). In contrast to the increasing ST with increasing molecular volume V_m as observed for the halide series, the ST decreases within these pairs with increasing molecular volume, i.e., with increasing number of noncoordinating CF_x groups (ST: $[MeOSO_3]^- > [TfO]^-$, $[Tf_2N]^- > [Pf_2N]^-$, $[PF_6]^- > [FAP]^-$). This decrease of ST with V_m is mainly ascribed to a decrease in Coulomb attraction in the bulk (i.e., a decrease in cohesive energy) as it was outlined in the Introduction. Because of the small dispersive contributions in case of the perfluorinated anions, the Coulombic contributions, which depend on the distance between the positive and negative centers of charge, are dominating. Therefore, an increase in anion size leads to an overall decrease in attractive interaction and to reduced ST values. The weakly polarizable CF_x groups of the anions do not allow for similar compensation effects as pointed out for the halide series. Apart from changes of the cohesive energy in the bulk, an influence of molecular orientation effects could also play a significant role for these anions. As witnessed by ARXP spectra of the ILs, a moderate increase in F 1s intensity with increasing surface sensitivity is observed in all cases.[40] Thus, the anions preferentially orient themselves at the surface in a way to expose the terminal CF_3 groups to the vacuum. Taking into account the weak attractive (or even repulsive) interaction between these groups, the reduced ST seems to be related to this orientation.

4. Summary and Conclusions

Various $[Tf_2N]^-$- and $[C_8C_1Im]^+$-based ILs were chosen to study the influence of the chemical nature of cation and anion on the density and the surface tension (at the liquid/air interface), which were determined by a vibrating tube densimeter and the pendant drop method, respectively. The influence of the alkyl chain length at the imidazolium ring was studied for the $[C_nC_1Im][Tf_2N]$ series ($n = 1, 2, 4, 6, 8, 10, 12$). With increasing chain length, a decrease in density is observed. The surface tension also decreases with increasing chain length, but reaches a plateau for $n = 8$. This initial increase is attributed to an increasing enrichment of the alkyl chains at the IL surface, as evidenced by angle-resolved XPS measurements. Thereby, the nonfunctionalized side chains tend to stick out toward the gas phase/vacuum, forming an aliphatic overlayer above a polar sublayer consisting of the imidazolium rings and the anions. With increasing alkyl chain length the distance between the polar sublayer and the outer surface increases. Therefore, for the longer alkyl chains the Coulombic interactions contribute less to the surface tension as compared to shorter alkyl chains.

By functionalizing the side chain with ethylene glycol groups ($[Me(EG)_2C_1Im][Tf_2N]$), a higher density and surface tension was found in comparison to the nonfunctionalized chain of the same length. This observation is attributed to the formation of inter- and intramolecular H-bonds between the oxygen atoms in the side chain and the acidic hydrogen atoms at the imidazolium ring, leading to a higher packing density. Furthermore, as again deduced from angle-resolved XPS measurements, these H-bonds lead to a loss of preferential orientation; i.e., no enrichment of the functionalized chains at the IL surface is found in these ethylene glycol functionalized ionic liquids.

The systematic variation of the anion in various $[C_8C_1Im]^+$-based ILs yields an overall increase of the density with increasing molecular weight of the anion. Only the anions Br^-, I^-, $[PF_6]^-$, and $[B(CN)_4]^-$ do not follow this trend, which is attributed to their strictly spherical shape. Concerning the surface tension, no evident general trend was seen with the molecular volume of the anion. This was attributed to the complex nature of the surface tension, which depends not only on the strength of intermolecular interactions but also on the orientation of the ions at the surface. When comparing various $[C_8C_1Im]^+$-based ILs (excluding $[C_8C_1Im][B(CN)_4]$), the surface tensions were found to vary in range of 27.7−33.3 mN m^{-1}; in contrast, for $[C_2C_1Im][Tf_2N]$ and $[C_2C_1Im][BF_4]$ a much broader variation from 35.1 to 53.9 mN m^{-1} is observed. The smaller variation for the $[C_8C_1Im]^+$-based ILs is attributed to the octyl substituent at the cation and the resulting enrichment of this long alkyl chain at the IL surface. This leads to a much more aliphatic

character of the IL surface, to a lower contribution of the Coulombic interaction to the surface tension, and thus to a smaller dependence on the nature of the anion.

The observed behavior for all ILs studied herein can qualitatively be explained in a consistent way considering Langmuir's principle, namely that the surface composition is determined by the interplay of cohesive energy and surface orientation due to nonisotropic intermolecular interactions of specific chemical groups of cations and anions.

In the light of the somehow inconsistent and varying literature data on surface tensions of ILs that have been reported so far, it is noteworthy to mention that this study reports the largest set of IL surface tension data obtained with the same experimental method of pendant drop. More importantly, for the first time all ILs applied in the surface tension measurements have been checked for their molecular surface cleanliness from low volatile, surface-active contaminants (such as traces of laboratory grease or other impurities acting as surfactants) by using X-ray-induced photoelectron spectroscopy.

Acknowledgment. This work has been supported by the DFG through SPP 1191, grants STE 620/7-2, WA 1615/8-2, and FR 1709/9-1, by the Erlangen Graduate School in Advanced Optical Technologies (SAOT) within the German Excellence Initiative and by the Excellence Cluster "Engineering of Advanced Materials" granted to the University of Erlangen-Nuremberg. We also thank the Max-Buchner-Stiftung for financial support. We thank Dr. Pete Licence and Alasdair Taylor of the University of Nottingham for supplying the $[C_8C_1Im]I$ sample and Prof. Stefan Spange and Ralf Lungwitz of the University of Chemnitz for $[C_8C_1Im][NO_3]$. We also thank the Merck Co. for providing the $[C_8C_1Im][FAP]$ and the $[C_8C_1Im][B(CN)_4]$ sample and Iolitec, Denzlingen, for $[C_4C_1Pyrr][Tf_2N]$.

Supporting Information Available: In Table S1 all measured densities are listed. Table S2 contains the density, molecular volume, thermal expansion coefficient, and surface tension at 293.15 K for all studied ILs. In Figure S1 the N 1s spectra of $[C_4C_1Im][Tf_2N]$ and $[C_4C_1Pyrr][Tf_2N]$ are displayed. This material is available free of charge via the Internet at http://pubs.acs.org.

References and Notes

(1) *Ionic Liquids in Synthesis*; Wasserscheid, P., Welton, T., Eds.; Wiley-VCH: Weinheim, Germany, 2008.
(2) Plechkova, N. V.; Seddon, K. R. *Chem. Soc. Rev.* **2008**, *37*, 123.
(3) Minami, I. *Molecules* **2009**, *14*, 2286.
(4) Zhou, F.; Liang, Y. M.; Liu, W. M. *Chem. Soc. Rev.* **2009**, *38*, 2590.
(5) Han, X.; Armstrong, D. W. *Acc. Chem. Res.* **2007**, *40*, 1079.
(6) Berthod, A.; Ruiz-Angel, M.; Carda-Broch, S. *J. Chromatogr. A* **2008**, *1184*, 6.
(7) Stracke, M. P.; Ebeling, G.; Cataluna, R.; Dupont, J. *Energy Fuels* **2007**, *21*, 1695.
(8) Tempel, D. J.; Henderson, P. B.; Brzozowski, J. R.; Pearlstein, R. M.; Cheng, H. S. *J. Am. Chem. Soc.* **2008**, *130*, 400.
(9) Muldoon, M. J. *Dalton Trans.* **2010**, *39*, 337.
(10) Riisager, A.; Fehrmann, R.; Haumann, M.; Wasserscheid, P. *Eur. J. Inorg. Chem.* **2006**, 695.
(11) Gu, Y. L.; Li, G. X. *Adv. Synth. Catal.* **2009**, *351*, 817.
(12) Liu, H. T.; Liu, Y.; Li, J. H. *Phys. Chem. Chem. Phys.* **2010**, *12*, 1685.
(13) MacFarlane, D. R.; Forsyth, M.; Howlett, P. C.; Pringle, J. M.; Sun, J.; Annat, G.; Neil, W.; Izgorodina, E. I. *Acc. Chem. Res.* **2007**, *40*, 1165.
(14) Abbott, A. P.; McKenzie, K. J. *Phys. Chem. Chem. Phys.* **2006**, *8*, 4265.
(15) Slattery, J. M.; Daguenet, C.; Dyson, P. J.; Schubert, T. J. S.; Krossing, I. *Angew. Chem., Int. Ed.* **2007**, *46*, 5384.
(16) As it is also the case for the work presented here, in most investigations, rather interfacial tension values of ionic liquids in contact with air or an inert gas atmosphere have been measured. Due to the very low vapor pressure of aprotic ILs (generally, below 10^{-9} mbar at room temperature), the real surface tension of ILs in equilibrium solely with their own vapor phase is extremely difficult to be evaluated. However, as commonly used in most publications, we also adapt the term "surface tension" for the measured interfacial tension. The role of the gas atmosphere will be discussed later in the text.
(17) Law, G.; Watson, P. R. *Chem. Phys. Lett.* **2001**, *345*, 1.
(18) Dzyuba, S. V.; Bartsch, R. A. *ChemPhysChem* **2002**, *3*, 161.
(19) Carvalho, P. J.; Freire, M. G.; Marrucho, I. M.; Queimada, A. J.; Coutinho, J. A. P. *J. Chem. Eng. Data* **2008**, *53*, 1346.
(20) Zaitsau, D. H.; Kabo, G. J.; Strechan, A. A.; Paulechka, Y. U.; Tschersich, A.; Verevkin, S. P.; Heintz, A. *J. Phys. Chem. A* **2006**, *110*, 7303.
(21) Osada, R.; Hoshino, T.; Okada, K.; Ohmasa, Y.; Yao, M. *J. Chem. Phys.* **2009**, 130.
(22) Freire, M. G.; Carvalho, P. J.; Fernandes, A. M.; Marrucho, I. M.; Queimada, A. J.; Coutinho, J. A. P. *J. Colloid Interface Sci.* **2007**, *314*, 621.
(23) Fang, D. W.; Guan, W.; Tong, J.; Wang, Z. W.; Yang, J. Z. *J. Phys. Chem. B* **2008**, *112*, 7499.
(24) Ghatee, M. H.; Zolghadr, A. R. *Fluid Phase Equilib.* **2008**, *263*, 168.
(25) Santos, C. S.; Baldelli, S. *J. Phys. Chem. B* **2009**, *113*, 923.
(26) Zhou, Z. B.; Matsumoto, H.; Tatsumi, K. *ChemPhysChem* **2005**, *6*, 1324.
(27) Torrecilla, J. S.; Palomar, J.; Garcia, J.; Rodriguez, F. *J. Chem. Eng. Data* **2009**, *54*, 1297.
(28) Jiang, W.; Wang, Y. T.; Yan, T. Y.; Voth, G. A. *J. Phys. Chem. C* **2008**, *112*, 1132.
(29) Bhargava, B. L.; Balasubramanian, S.; Klein, M. L. *Chem. Commun.* **2008**, 3339.
(30) Solutskin, E.; Ocko, B. M.; Taman, L.; Kuzmenko, I.; Gog, T.; Deutsch, M. *J. Am. Chem. Soc.* **2005**, *127*, 7796.
(31) Fröba, A. P.; Kremer, H.; Leipertz, A. *J. Phys. Chem. B* **2008**, *112*, 12420.
(32) Law, G.; Watson, P. R. *Langmuir* **2001**, *17*, 6138.
(33) Martino, W.; de la Mora, J. F.; Yoshida, Y.; Saito, G.; Wilkes, J. *Green Chem.* **2006**, *8*, 390.
(34) Larriba, C.; Yoshida, Y.; de la Mora, J. F. *J. Phys. Chem. B* **2008**, *112*, 12401.
(35) Rusanov, A. I.; Prokhorov, V. A. *Interfacial tensiometry*; Elsevier: Amsterdam, 1996.
(36) Langmuir, I. *Chem. Rev.* **1930**, *6*, 451.
(37) Langmuir, I. *Surface Chemistry (Nobel Lecture, 1932)*; Elsevier Publishing Co.: Amsterdam, 1966.
(38) Steinrück, H. P. *Surf. Sci.* **2010**, *604*, 481.
(39) Lovelock, K. R. J.; Kolbeck, C.; Cremer, T.; Paape, N.; Schulz, P. S.; Wasserscheid, P.; Maier, F.; Steinrück, H. P. *J. Phys. Chem. B* **2009**, *113*, 2854.
(40) Kolbeck, C.; Cremer, T.; Lovelock, K. R. J.; Paape, N.; Schulz, P. S.; Wasserscheid, P.; Maier, F.; Steinrück, H. P. *J. Phys. Chem. B* **2009**, *113*, 8682.
(41) Kuhlmann, E.; Himmler, S.; Giebelhaus, H.; Wasserscheid, P. *Green Chem.* **2007**, *9*, 233.
(42) Gottfried, J. M.; Maier, F.; Rossa, J.; Gerhard, D.; Schulz, P. S.; Wasserscheid, P.; Steinrück, H. P. *Z. Phys. Chem.* **2006**, *220*, 1439.
(43) Kolbeck, C.; Killian, M.; Maier, F.; Paape, N.; Wasserscheid, P.; Steinruck, H. P. *Langmuir* **2008**, *24*, 9500.
(44) Maier, F.; Cremer, T.; Kolbeck, C.; Lovelock, K. R. J.; Paape, N.; Schulz, P. S.; Wasserscheidc, P.; Steinrück, H. P. *Phys. Chem. Chem. Phys.* **2010**, *12*, 1905.
(45) Lemmon, E. W.; Span, R. *J. Chem. Eng. Data* **2006**, *51*, 785.
(46) Tokuda, H.; Hayamizu, K.; Ishii, K.; Susan, M. A. B. H.; Watanabe, M. *J. Phys. Chem. B* **2005**, *109*, 6103.
(47) Tariq, M.; Forte, P. A. S.; Gomes, M. F. C.; Lopes, J. N. C.; Rebelo, L. P. N. *J. Chem. Thermodyn.* **2009**, *41*, 790.
(48) Wandschneider, A.; Lehmann, J. K.; Heintz, A. *J. Chem. Eng. Data* **2008**, *53*, 596.
(49) Troncoso, J.; Cerdeirina, C. A.; Navia, P.; Sanmamed, Y. A.; Gonzalez-Salgado, D.; Romani, L. *J Phys Chem Lett* **2010**, *1*, 211.
(50) Pereiro, A. B.; Legido, J. L.; Rodriguez, A. *J. Chem. Thermodyn.* **2007**, *39*, 1168.
(51) Sanchez, L. G.; Espel, J. R.; Onink, F.; Meindersma, G. W.; de Haan, A. B. *J. Chem. Eng. Data* **2009**, *54*, 2803.
(52) Fandino, O.; Lopez, E. R.; Lugo, L.; Fernandez, J. *Fluid Phase Equilib.* **2010**, *296*, 30.
(53) *Chemical Properties Handbook*; Yaws, C. L., Ed.; McGraw-Hill: New York, 1999; pp 779.
(54) Wang, Y. T.; Voth, G. A. *J. Am. Chem. Soc.* **2005**, *127*, 12192.

(55) Lopes, J. N. A. C.; Padua, A. A. H. *J. Phys. Chem. B* **2006**, *110*, 3330.
(56) Glasser, L. *Thermochim. Acta* **2004**, *421*, 87.
(57) Himmler, S.; Hormann, S.; van Hal, R.; Schulz, P. S.; Wasserscheid, P. *Green Chem.* **2006**, *8*, 887.
(58) Lopez, E. R.; Daridon, J. L.; Plantier, F.; Boned, C.; Fernandez, J. *Int. J. Thermophys.* **2006**, *27*, 1354.
(59) Smith, G. D.; Borodin, O.; Li, L. Y.; Kim, H.; Liu, Q.; Bara, J. E.; Gin, D. L.; Nobel, R. *Phys. Chem. Chem. Phys.* **2008**, *10*, 6301.
(60) Fei, Z. F.; Ang, W. H.; Zhao, D. B.; Scopelliti, R.; Zvereva, E. E.; Katsyuba, S. A.; Dyson, P. J. *J. Phys. Chem. B* **2007**, *111*, 10095.
(61) Jin, H.; O'Hare, B.; Dong, J.; Arzhantsev, S.; Baker, G. A.; Wishart, J. F.; Benesi, A. J.; Maroncelli, M. *J. Phys. Chem. B* **2008**, *112*, 81.
(62) Gomez, E.; Gonzalez, B.; Dominguez, A.; Tojo, E.; Tojo, J. *J. Chem. Eng. Data* **2006**, *51*, 696.
(63) Liu, W. W.; Zhao, T. Y.; Zhang, Y. M.; Wang, H. P.; Yu, M. F. *J. Solution Chem.* **2006**, *35*, 1337.
(64) MacLeod, D. B. *Trans. Faraday Soc.* **1923**, *19*, 38.
(65) Sudgen, S. *J. Chem. Soc.* **1924**, *125*, 32.
(66) Fröba, A. P.; Leipertz, A. *J. Chem. Eng. Data* **2007**, *52*, 1803.
(67) Rilo, E.; Pico, J.; Garcia-Garabal, S.; Varela, L. M.; Cabeza, O. *Fluid Phase Equilib.* **2009**, *285*, 83.
(68) Sung, J.; Jeon, Y.; Kim, D.; Iwahashi, T.; Seki, K.; Iimori, T.; Ouchi, Y. *Colloids Surf. A* **2006**, *284*, 84.
(69) Liu, W. W.; Cheng, L. Y.; Zhang, Y. M.; Wang, H. P.; Yu, M. F. *J. Mol. Liq.* **2008**, *140*, 68.
(70) Ries, L. A. S.; do Amaral, F. A.; Matos, K.; Martini, E. M. A.; de Souza, M. O.; de Souza, R. F. *Polyhedron* **2008**, *27*, 3287.
(71) Modaressi, A.; Sifaoui, H.; Mielcarz, M.; Domanska, U.; Rogalski, M. *Colloids Surf. A* **2007**, *302*, 181.
(72) Fröba, A. P.; Wasserscheid, P.; Gerhard, D.; Kremer, H.; Leipertz, A. *J. Phys. Chem. B* **2007**, *111*, 12817.
(73) Rivera-Rubero, S.; Baldelli, S. *J. Phys. Chem. B* **2006**, *110*, 15499.
(74) Cuadrado-Prado, S.; Dominguez-Perez, M.; Rilo, E.; Garcia-Garabal, S.; Segade, L.; Franjo, C.; Cabeza, O. *Fluid Phase Equilib.* **2009**, *278*, 36.
(75) Seddon, K. R.; Stark, A.; Torres, M. J. *Pure Appl. Chem.* **2000**, *72*, 2275.
(76) Baldelli, S. *J. Phys. Chem. B* **2003**, *107*, 6148.
(77) Hashimoto, H.; Ohno, A.; Nakajima, K.; Suzuki, M.; Tsuji, H.; Kimura, K. *Surf. Sci.* **2010**, *604*, 464.
(78) Koddermann, T.; Paschek, D.; Ludwig, R. *ChemPhysChem* **2008**, *9*, 549.
(79) Lockett, V.; Sedev, R.; Bassell, C.; Ralston, J. *Phys. Chem. Chem. Phys.* **2008**, *10*, 1330.
(80) Iimori, T.; Iwahashi, T.; Ishii, H.; Seki, K.; Ouchi, Y.; Ozawa, R.; Hamaguchi, H.; Kim, D. *Chem. Phys. Lett.* **2004**, *389*, 321.
(81) Rivera-Rubero, S.; Baldelli, S. *J. Phys. Chem. B* **2006**, *110*, 4756.
(82) Ohno, A.; Hashimoto, H.; Nakajima, K.; Suzuki, M.; Kimura, K. *J. Chem. Phys.* **2009**, 130.
(83) Bowers, J.; Vergara-Gutierrez, M. C.; Webster, J. R. P. *Langmuir* **2004**, *20*, 309.
(84) Deyko, A.; Lovelock, K. R. J.; Corfield, J. A.; Taylor, A. W.; Gooden, P. N.; Villar-Garcia, I. J.; Licence, P.; Jones, R. G.; Krasovskiy, V. G.; Chernikova, E. A.; Kustov, L. M. *Phys. Chem. Chem. Phys.* **2009**, *11*, 8544.
(85) Muhammad, A.; Mutalib, M. I. A.; Wilfred, C. D.; Murugesan, T.; Shafeeq, A. *J. Chem. Thermodyn.* **2008**, *40*, 1433.
(86) Cremer, T.; Kolbeck, C.; Lovelock, K. R. J.; Paape, N.; Wolfel, R.; Schulz, P. S.; Wasserscheid, P.; Weber, H.; Thar, J.; Kirchner, B.; Maier, F.; Steinruck, H. P. *Chem.—Eur. J.* **2010**, *16*, 9018.
(87) Mortimer, C. E. *Chemistry*; Wadsworth Publishing: Belmont, CA, 1986.
(88) Jaswal, S. S.; Sharma, T. P. *J. Phys. Chem. Solids* **1973**, *34*, 509.
(89) Hajj, F. *J. Chem. Phys.* **1966**, *44*, 4618.
(90) Boswarva, I. M.; Murthy, C. S. N. *J. Phys. Chem. Solids* **1981**, *42*, 109.
(91) Note that the increase of the ST as a function of the molecular volume in both subgroups is very similar as indicated by the identical slopes of the dashed red and green lines in Figure 4b which could indicate similar mechanisms behind.
(92) Smart, B. E. *J. Fluorine Chem.* **2001**, *109*, 3.
(93) Huddleston, J. G.; Visser, A. E.; Reichert, W. M.; Willauer, H. D.; Broker, G. A.; Rogers, R. D. *Green Chem.* **2001**, *3*, 156.
(94) Kilaru, P.; Baker, G. A.; Scovazzo, P. *J. Chem. Eng. Data* **2007**, *52*, 2306.
(95) Rebelo, L. P. N.; Lopes, J. N. C.; Esperanca, J. M. S. S.; Filipe, E. *J. Phys. Chem. B* **2005**, *109*, 6040.
(96) Klomfar, J.; Souckova, M.; Patek, J. *J. Chem. Thermodyn.* **2010**, *42*, 323.
(97) Restolho, J.; Mata, J. L.; Saramago, B. *J. Colloid Interface Sci.* **2009**, *340*, 82.
(98) Fletcher, S. I.; Sillars, F. B.; Hudson, N. E.; Hall, P. J. *J. Chem. Eng. Data* **2010**, *55*, 778.

JP1068413

Table S1: Density ρ for all investigated ionic liquids in dependence on temperature.

ρ / g·cm^{-3}								
		T / K						
cation	anion	**278.15**	**283.15**	**288.15**	**293.15**	**298.15**	**303.15**	**308.15**
$[C_1C_1Im]^+$	$[Tf_2N]^-$	-	-	-	1.58263	1.56729	1.56344	1.55855
$[C_2C_1Im]^+$	$[Tf_2N]^-$	1.53882	1.53371	1.52861	1.52353	1.51845	1.51341	1.50839
$[C_4C_1Im]^+$	$[Tf_2N]^-$	1.45451	1.44971	1.44490	1.44007	1.43530	1.43052	1.42576
$[C_6C_1Im]^+$	$[Tf_2N]^-$	1.38329	1.37857	1.37384	1.36913	1.36442	1.35972	1.35504
$[C_8C_1Im]^+$	$[Tf_2N]^-$	1.32859	1.32402	1.31960	1.31515	1.31073	1.30630	1.30188
$[C_{10}C_1Im]^+$	$[Tf_2N]^-$	1.28751	1.28305	1.27861	1.27430	1.27001	1.26570	1.26141
$[C_{12}C_1Im]^+$	$[Tf_2N]^-$	1.26082	1.25647	1.25211	1.24777	1.24355	1.23936	1.23517
$[C_4C_1Pyrr]^+$	$[Tf_2N]^-$	1.41214	1.40759	1.40318	1.39876	1.39435	1.38994	1.38555
$[Me(EG)_2C_1Im]^+$	$[Tf_2N]^-$	1.47481	1.46986	1.46489	1.45994	1.45499	1.45007	1.44515
$[C_2C_1Im]^+$	$[BF_4]^-$	1.29501	1.29116	1.28730	1.28346	1.27965	1.27585	1.27207
$[C_8C_1Im]^+$	Br^-	1.18277	1.17940	1.17604	1.17269	1.16932	1.16589	1.16236
$[C_8C_1Im]^+$	I^-	1.32021	1.31647	1.31269	1.30882	1.30482	1.30095	1.29732
$[C_8C_1Im]^+$	$[NO_3]^-$	1.07815	1.07473	1.07132	1.06819	1.06507	1.06295	1.05884
$[C_8C_1Im]^+$	$[BF_4]^-$	1.11308	1.10959	1.10611	1.10258	1.09918	1.09583	1.09246
$[C_8C_1Im]^+$	$[PF_6]^-$	1.25144	1.24720	1.24313	1.23927	1.23540	1.23154	1.22768
$[C_8C_1Im]^+$	$[B(CN)_4]^-$	0.98915	0.98558	0.98206	0.97853	0.97502	0.97152	0.96803
$[C_8C_1Im]^+$	$[MeOSO_3]^-$	1.12315	1.11982	1.11649	1.11313	1.10984	1.10662	1.10339
$[C_8C_1Im]^+$	$[Pf_2N]^-$	1.41593	1.41095	1.40595	1.40096	1.39597	1.39116	1.38633
$[C_8C_1Im]^+$	$[FAP]^-$	1.51812	1.51271	1.50731	1.50208	1.49688	1.49169	1.48648

Table S2: Density ρ, molecular volume V_m, thermal expansion coefficient α_p, and surface tension σ at 293.15 K for all investigated ILs.

cation	anion	ρ / g cm^{-3}	V_m / nm^3	α_p / 10^{-4} K^{-1}	σ / mN m^{-1}
$[C_1C_1Im]^+$	$[Tf_2N]^-$	1.573	0.398	8.91	36.9
$[C_2C_1Im]^+$	$[Tf_2N]^-$	1.524[a]	0.427	6.66	35.6[a]
$[C_4C_1Im]^+$	$[Tf_2N]^-$	1.440	0.484	6.65	31.1
$[C_6C_1Im]^+$	$[Tf_2N]^-$	1.369	0.543	6.88	30.7
$[C_8C_1Im]^+$	$[Tf_2N]^-$	1.315	0.601	6.75	29.9
$[C_{10}C_1Im]^+$	$[Tf_2N]^-$	1.274	0.656	6.81	29.9
$[C_{12}C_1Im]^+$	$[Tf_2N]^-$	1.248	0.708	6.85	30.2
$[C_4C_1Pyrr]^+$	$[Tf_2N]^-$	1.399	0.502	6.32	32.7
$[Me(EG)_2C_1Im]^+$	$[Tf_2N]^-$	1.460	0.530	6.77	37.0
$[C_2C_1Im]^+$	$[BF_4]^-$	1.283	0.256	5.96	54.6
$[C_8C_1Im]^+$	Br^-	1.173	0.390	5.78	32.0
$[C_8C_1Im]^+$	I^-	1.309	0.409	5.87	33.1
$[C_8C_1Im]^+$	$[NO_3]^-$	1.068	0.400	6.00	33.7
$[C_8C_1Im]^+$	$[BF_4]^-$	1.103	0.425	6.24	31.2
$[C_8C_1Im]^+$	$[PF_6]^-$	1.239	0.456	6.36	32.9
$[C_8C_1Im]^+$	$[B(CN)_4]^-$	0.979	0.527	7.19	39.2
$[C_8C_1Im]^+$	$[MeOSO_3]^-$	1.113	0.457	5.92	30.4
$[C_8C_1Im]^+$	$[Pf_2N]^-$	1.401	0.682	7.05	28.0
$[C_8C_1Im]^+$	[FAP]$^-$	1.502	0.708	7.01	30.7

[a] Ref. [31]

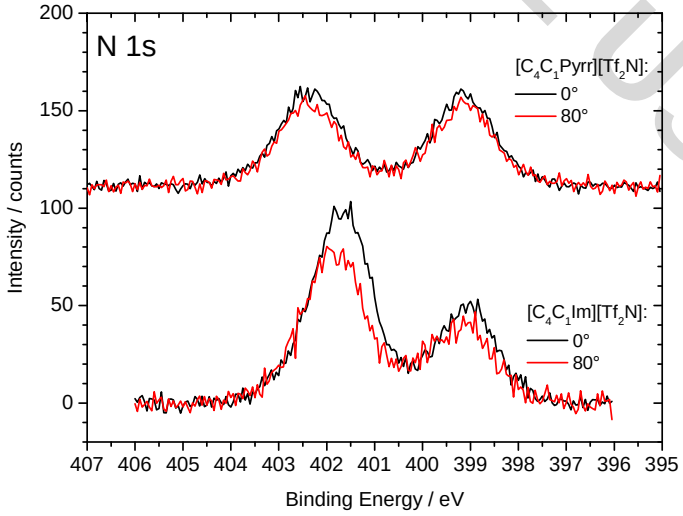

Figure S1: N 1s XP spectra of $[C_4C_1Im][Tf_2N]$ (bottom) and $[C_4C_1Pyrr][Tf_2N]$ (top) taken under 0° (black, more bulk sensitive) and 80° (red, more surface sensitive) emission angle with respect to the surface normal.